Electronic Supplementary Information

Cyclometallated iridium complexes inducing natural product like paraptotic cell death: Synthesis, structure and mechanistic aspects

Suman Kumar Tripathy,[a,†] Umasankar De,[b,†] Niranjan Dehury,[a] Paltan Laha,[a] Manas Kumar Panda,[c] Hyung Sik Kim[b,*] and Srikanta Patra[a,*]

[a]School of Basic Sciences, Indian Institute of Technology Bhubaneswar, Bhubaneswar-751007, India. Tel: 0674 2576053, E-mail: srikanta@iitbbs.ac.in,

[b]Division of Toxicology, School of Pharmacy, Sungkyunkwan University, Suwon, Gyeonggi-do, Republic of Korea. Tel: +82-31-290-7789, E-mail: hkims@skku.edu.

[c]National Institute for Interdisciplinary Science and Technology (NIIST), Thiruvananthapuram – 695 019, Kerala, India

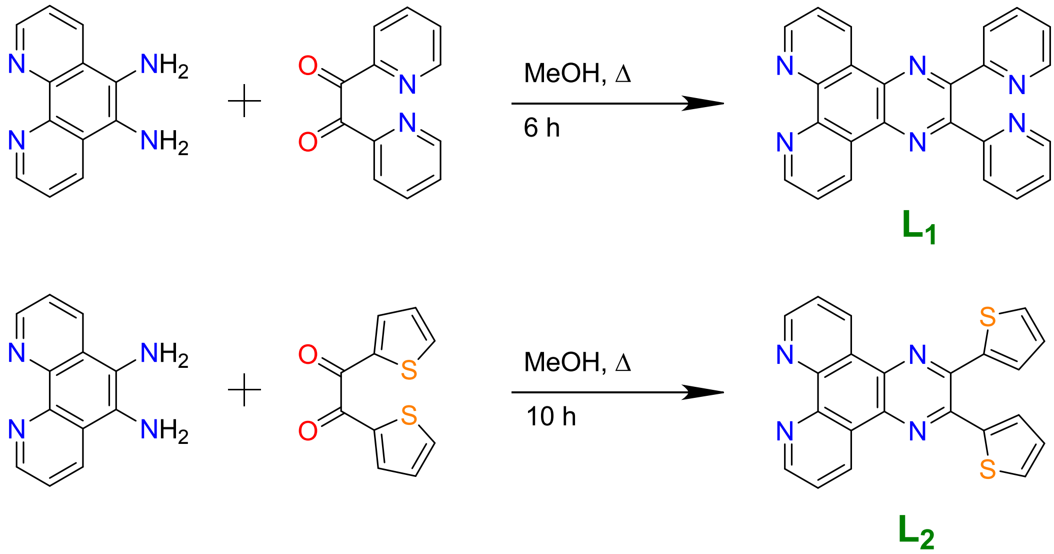

Scheme S1. Schematic representation for the preparation of the ligands $\mathbf{L_1}$ and $\mathbf{L_2}$.

Table TS1. Selected crystallographic data for complex **5.** $3C_7H_8$ and **6**. C_7H_8.

	5.$3C_7H_8$	**6**. C_7H_8
emperical formula	$C_{113}H_{88}F_{12}Ir_2N_{12}P_2S_4$	$C_{43}H_{37}ClF_6IrN_6P$
Fw	2416.53	1010.43
radiation	MoK_α	MoK_α
wavelength (Å)	0.71073	0.71073
temp./ K	110 (2)	110(2)
crystal system	Trigonal	Triclinic
space group	R - 3	P - 1
a/Å	49.3580(8)	8.7494(7)
b/Å	49.3580(8)	12.8229(9)
c/Å	11.9179(19)	18.0175(14)
α(deg)	90.00	95.984(2)
β(deg)	90.00	92.269(2)
γ(deg)	120.00	92.255(2)
V/ Å^3	25145(9)	2006.9(3)
crystal size (mm)	0.33 x 0.22 x 0.20	0.10 x 0.08 x 0.06
Z	9	2
μ / mm^{-1}	2.554	3.501
D_{calcd} / g cm^{-3}	1.436	1.672
F(000)	10854	1000
θ range	2.18-23.21	2.06-28.44
data/restraints/parameters	13028/129/622	8693/0/529
R1,wR2 [I>2σ(I)]	0.0588, 0.1132	0.0693, 01017
R1,wR2 (all data)	0.1132	0.1017,
largest diff. peak hole (eÅ^{-3})	2.322, -1.115	2.279, -2.21

Table TS2. Important bond distances (Å) and bond angles (°) for **5**. $3C_7H_8$ and **6**. C_7H_8

Bond lengths (Å)			
5.$3C_7H_8$		**6**. C_7H_8	
Ir1-N1	2.138(5)	Ir1-N1	2.133(7)
Ir1-N2	2.144(5)	Ir1-N2	2.114(7)
Ir1-N5	2.048(5)	Ir1-C25	2.172(9)
Ir1-N6	2.046(5)	Ir1-C26	2.158(9)
Ir1-C33	2.006(6)	Ir1-C27	2.123(9)
Ir1-C45	2.010(6)	Ir1-C28	2.171(10)
		Ir1-C29	2.176(10)
		Ir1-Cl1	2.401(2)
		Ir-$C_{centroid}$	1.790
Bond angles (°)			
5.$3C_7H_8$		**6.** C_7H_8	
N1-Ir1-N2	77.27(17)	N1-Ir1-Cl1	84.9(2)
C33-Ir1-N3	80.9(2)	N2-Ir1-Cl1	86.71(19)
C45-Ir1-N4	80.5(2)	N1-Ir1-N2	77.4(3)

Table TS3. UV-Vis spectral and electrochemical data[a] for complexes **1 – 6** recorded in CH_3CN at room temperature.

Complexes	λ_{max}/nm(ε / M^{-1} cm^{-1})	E_{298}^{o} [V][b]					
		E_{ox2}	E_{ox1}	E_{red1}	E_{red2}	E_{red3}	E_{red4}
1	267 (82500), 365 (22500)	—	1.18 V	-0.82	-1.41	-1.96	—
2	272 (75700), 360 (22000), 477 (670)	1.14	0.79 V	-0.81	-1.43	-1.96	—
3	246 (77680), 270 (77670), 348 (23200), 363 (22300), 446 (790)	—	1.44 V	-0.8	-1.07	-1.38	-1.94
4	260 (69100), 392 (26250)	1.12	0.85 V	-0.84	-1.08	-1.94	—
5	253 (61000), 271 (59200), 378 (19300)	—	1.09 V	-0.99	-1.14	-1.72	—
6	213 (27300), 285 (34000), 360 (10800)		1.61 V	-1.09	-1.43	-1.82	—

[a]From cyclic voltammetry in CH_3CN/ 0.1M Et_4NClO_4 at 50 mV s^{-1}. [b]Potentials in V *versus* Ag/AgCl, referenced to Fc^+/Fc ($E_{½}$ = + 0.18 V) as internal standard.

Figure S1. Positive ion ESI mass spectra of complexes **1 - 6.**

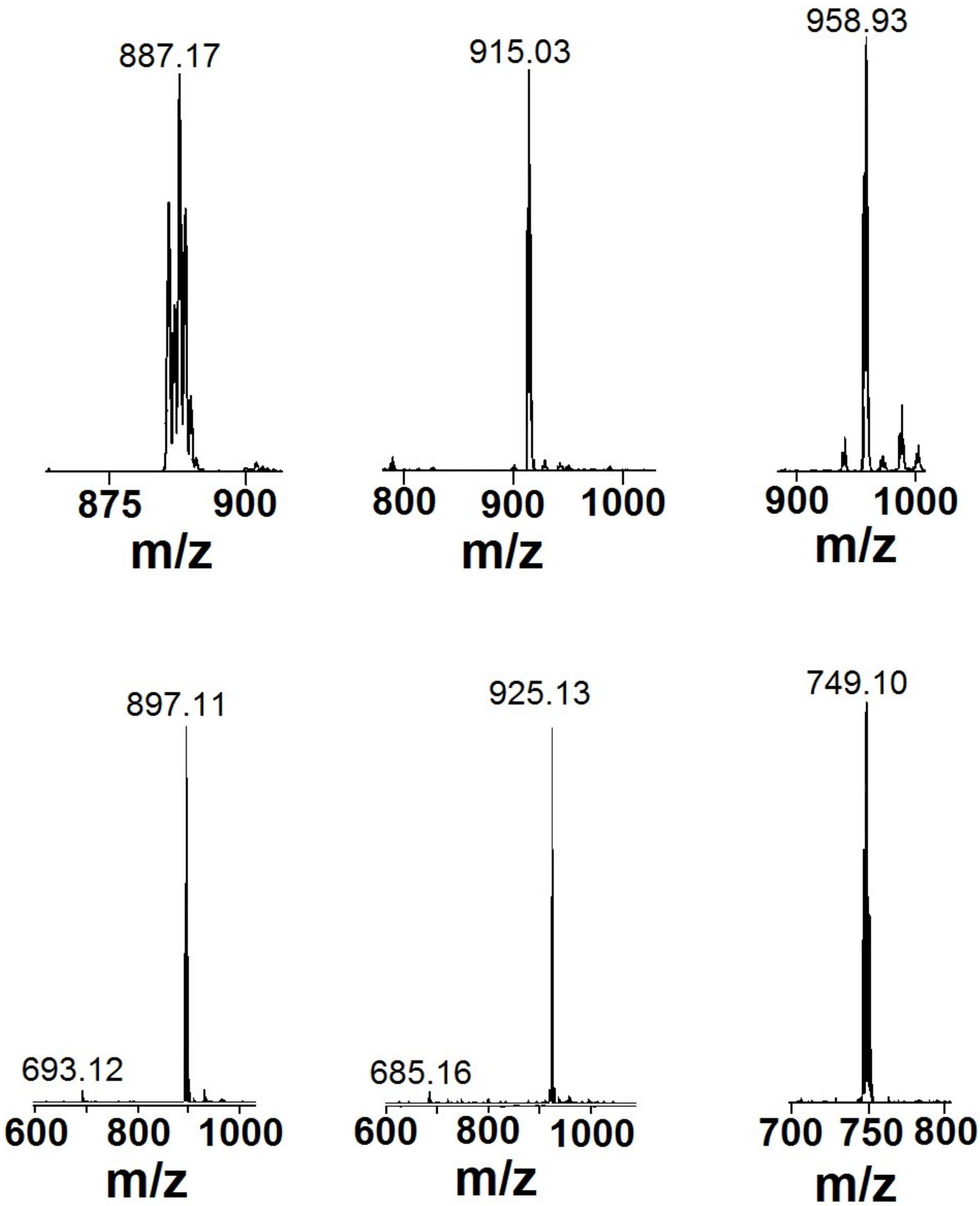

Figure S2. (a) ^{1}H and (b) ^{13C} NMR spectra of complex **1** in $(CD_3)_2SO$.

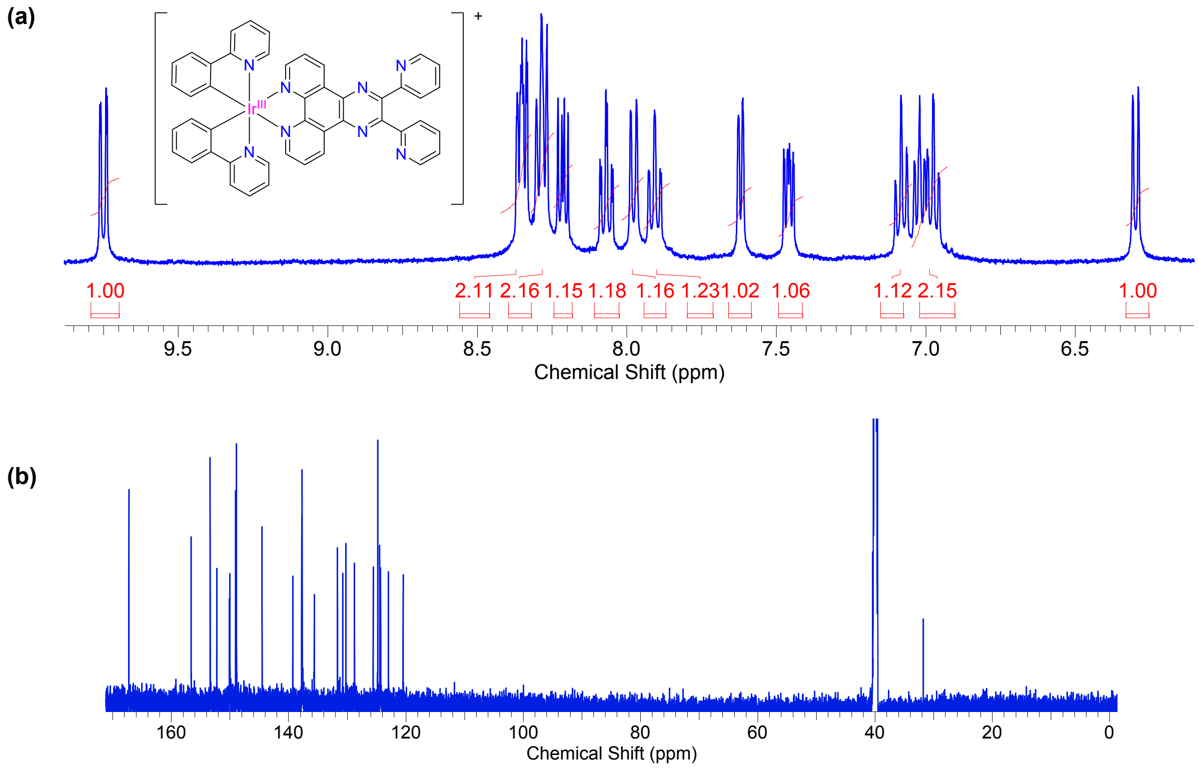

Figure S3. (a) ^{1}H and (b) ^{13}C NMR spectra of complex **2** in $(CD_3)_2SO$.

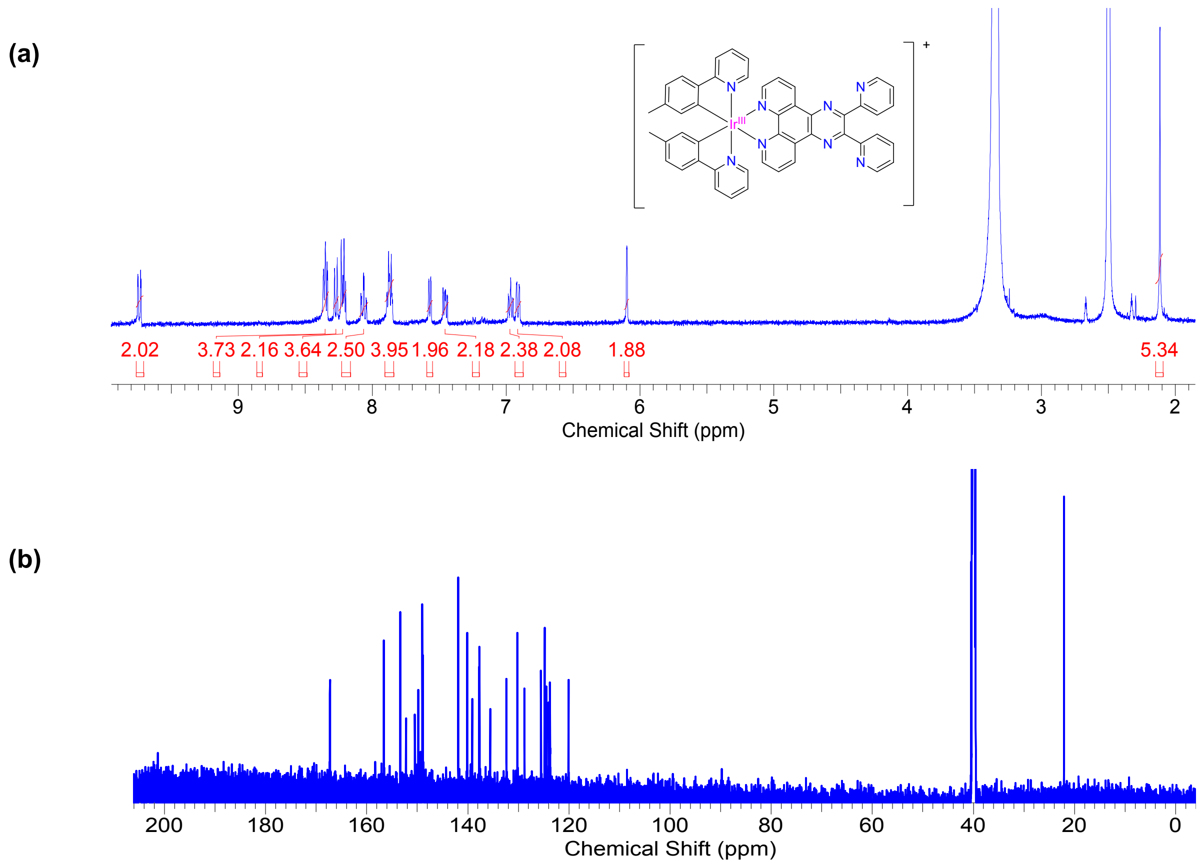

Figure S4. (a) ^{1}H and (b) ^{13C} NMR spectra of complex **3** in $(CD_3)_2SO$.

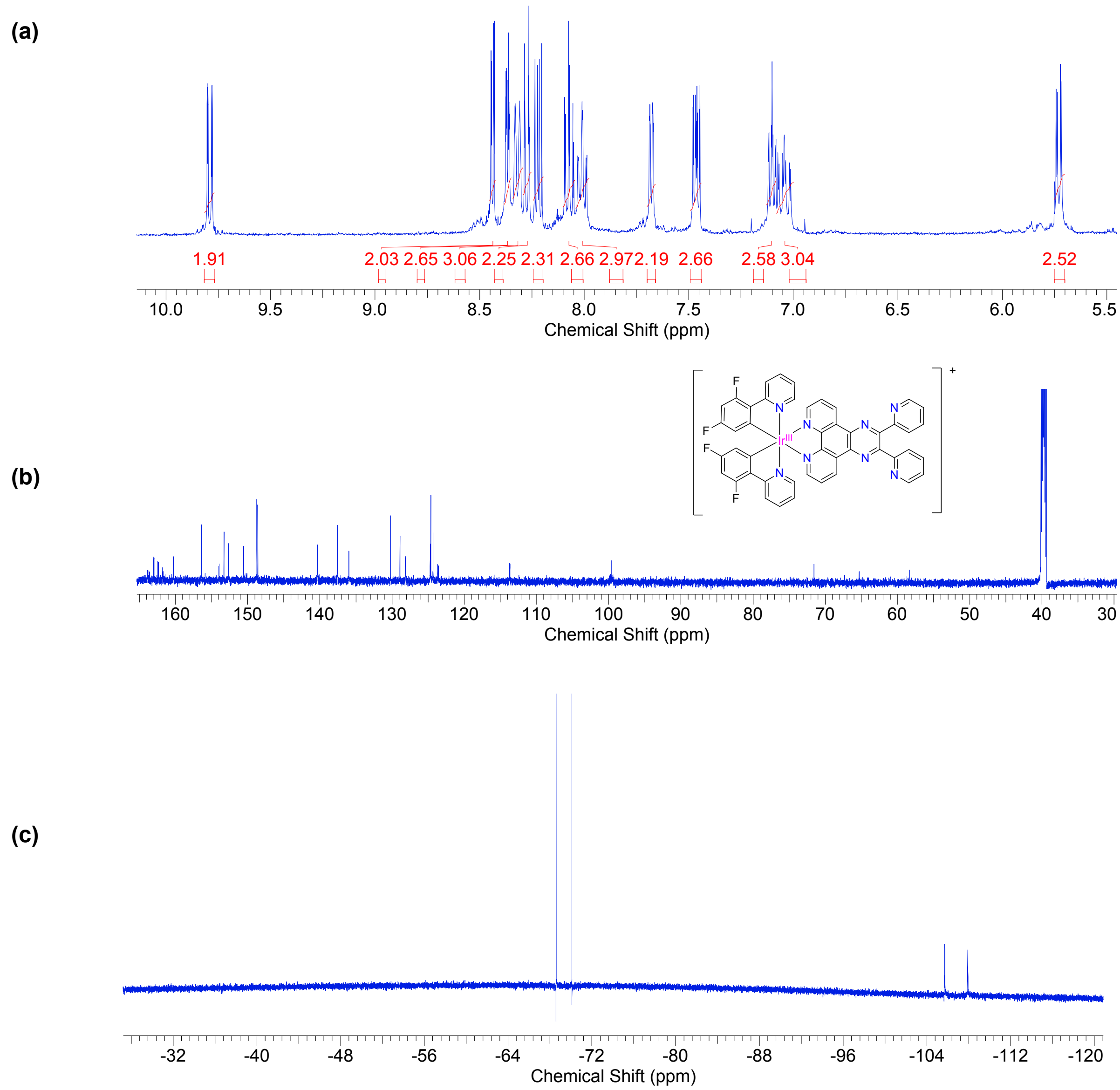

Figure S5. (a) ^{1}H and (b) ^{13C} NMR spectra of complex **4** in $(CD_3)_2SO$.

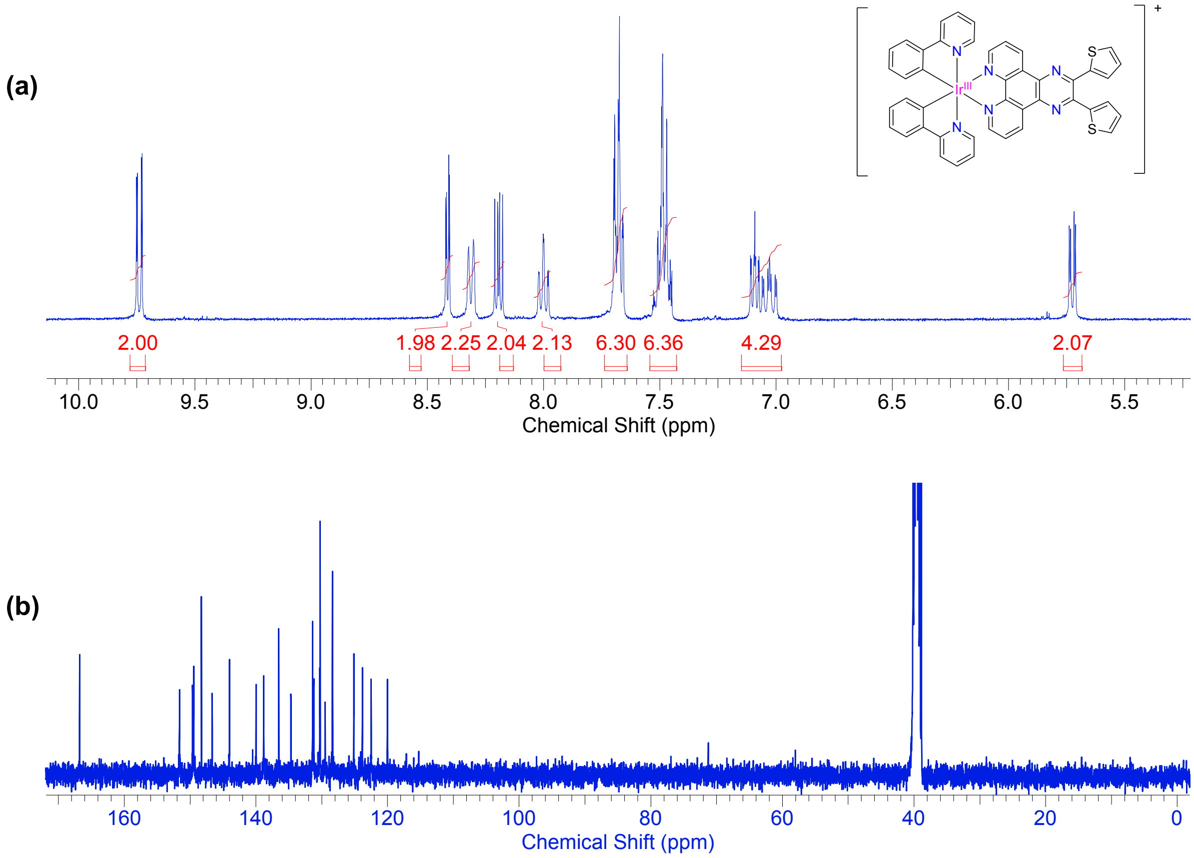

Figure S6. (a) ^{1}H and (b) ^{13}C NMR spectra of complex **5** in $(CD_3)_2SO$.

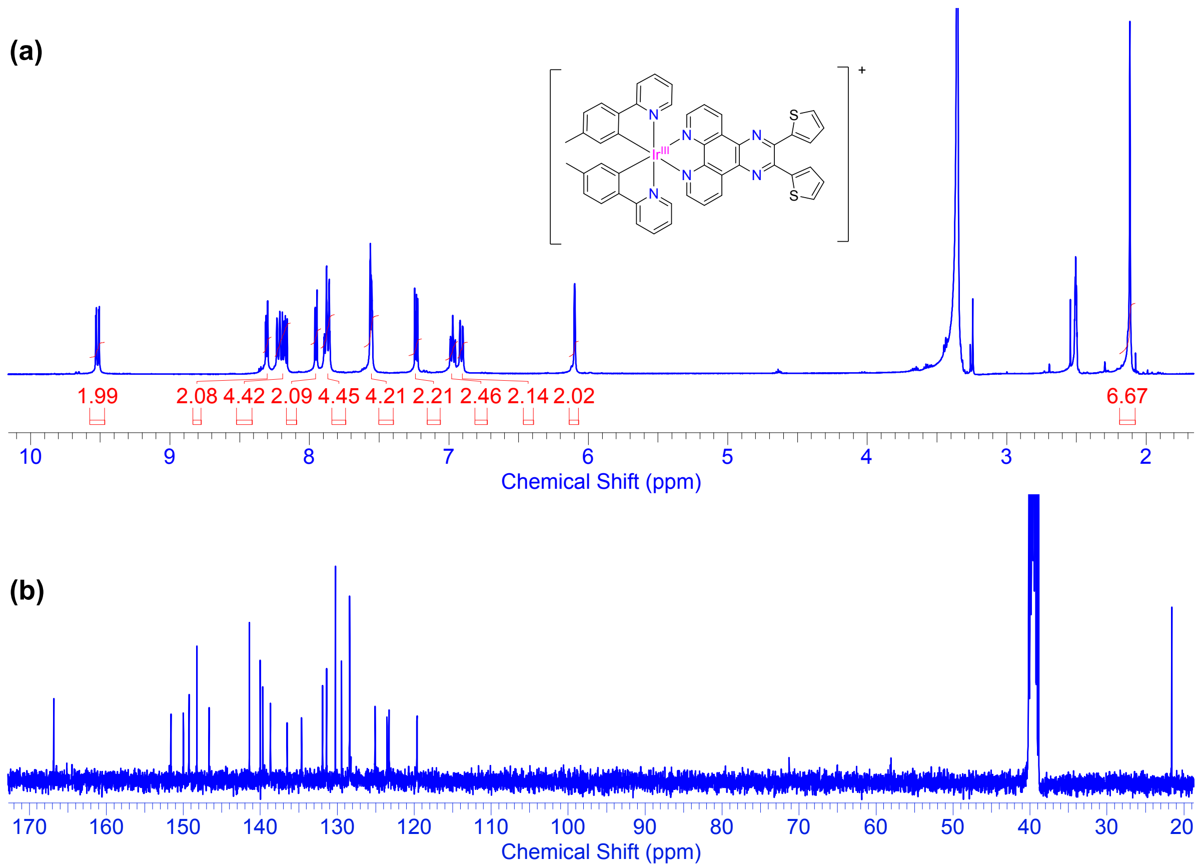

Figure S7. (a) ^{1}H and (b) ^{13C} NMR spectra of complex **6** in $(CD_3)_2SO$.

(a)

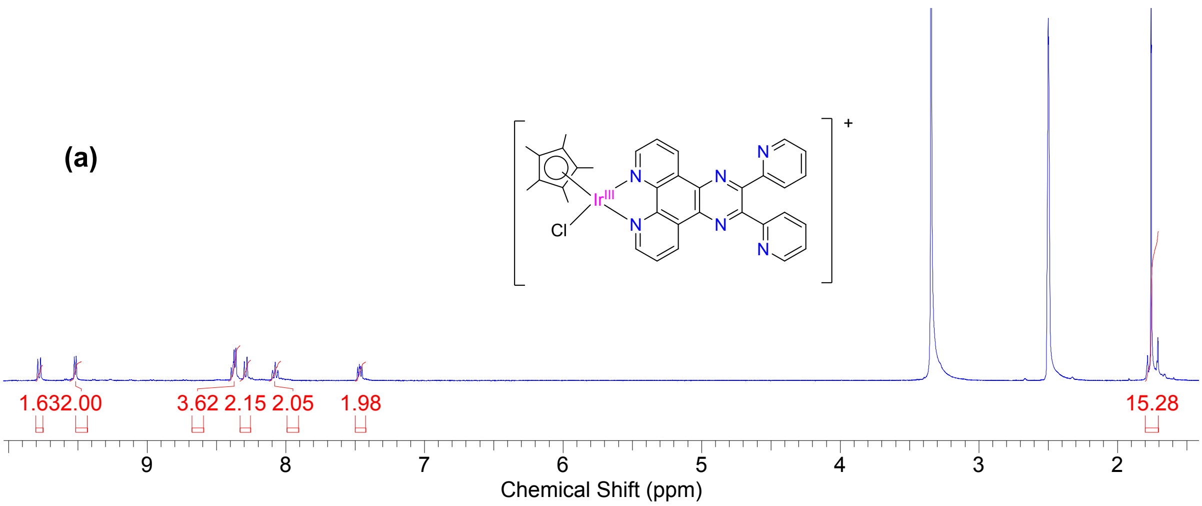

(b)

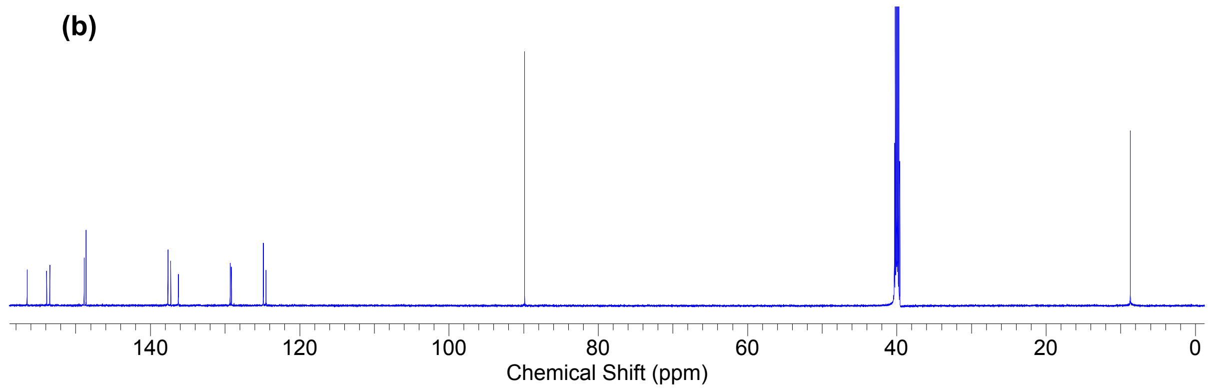

Figure S8. UV-Vis spectra of the complexes **1 - 6** recorded in CH_3CN at room temperature.

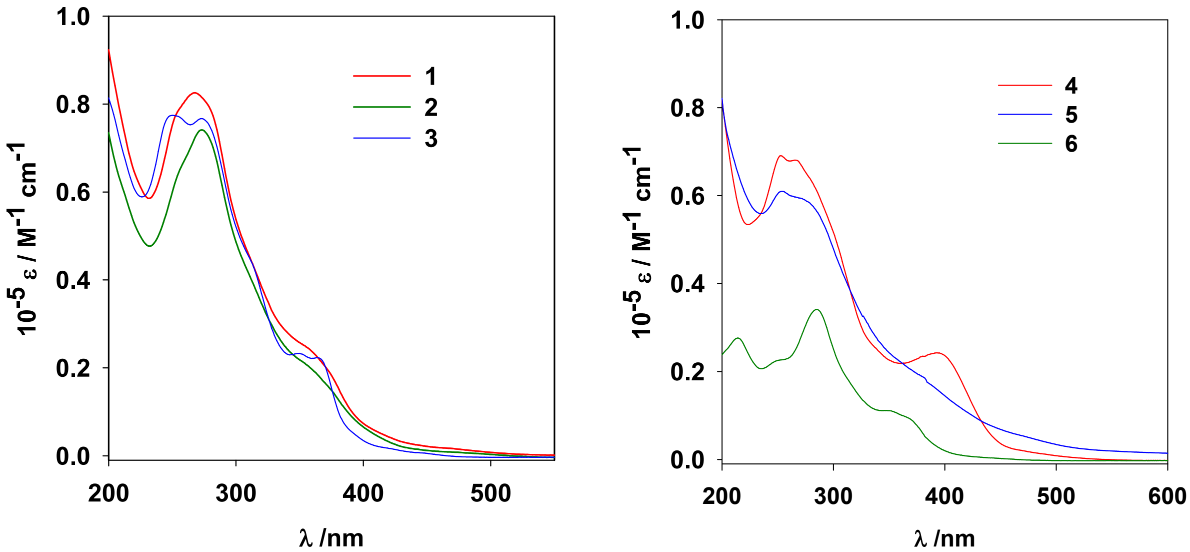

Figure S9. Cyclic voltammograms of the complexes **1 - 6** recorded in CH_3CN/0.1M Et_4NClO_4 *versus* Ag/AgCl (scan rate 50 mV s^{-1}).

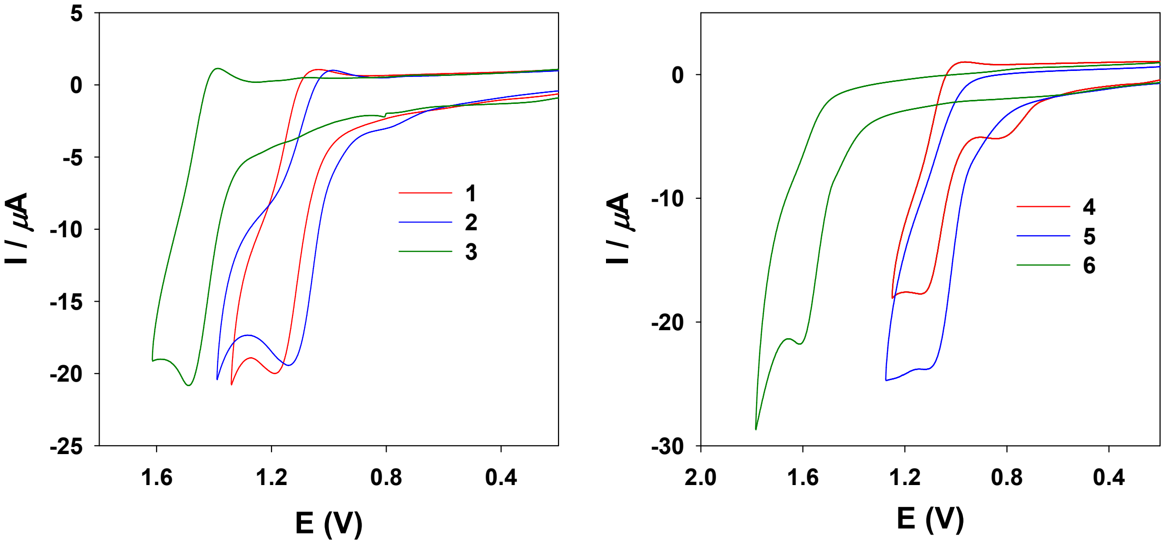

Figure S10. Dose dependent suppression of cell viability of complexes **1 – 6** towards human breast (MCF-7) cancer cell lines.

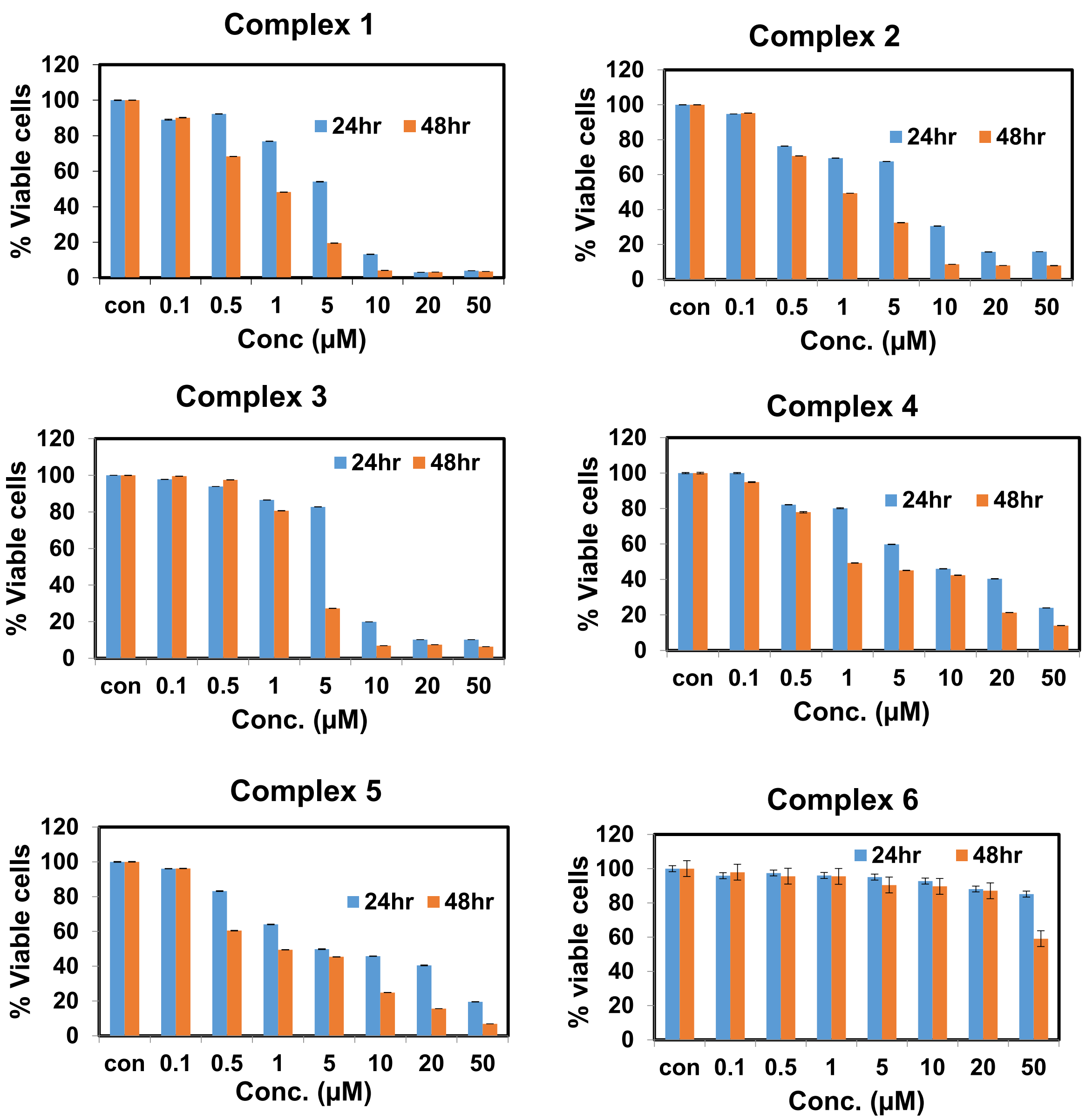

Figure S11. Flow cytometry results of MCF-7 cells incubated with blank medium and complexes **1** - **6** (5 µM) at 37 °C for 2 h. (excitation, 530 nm; emission, 585 nm).

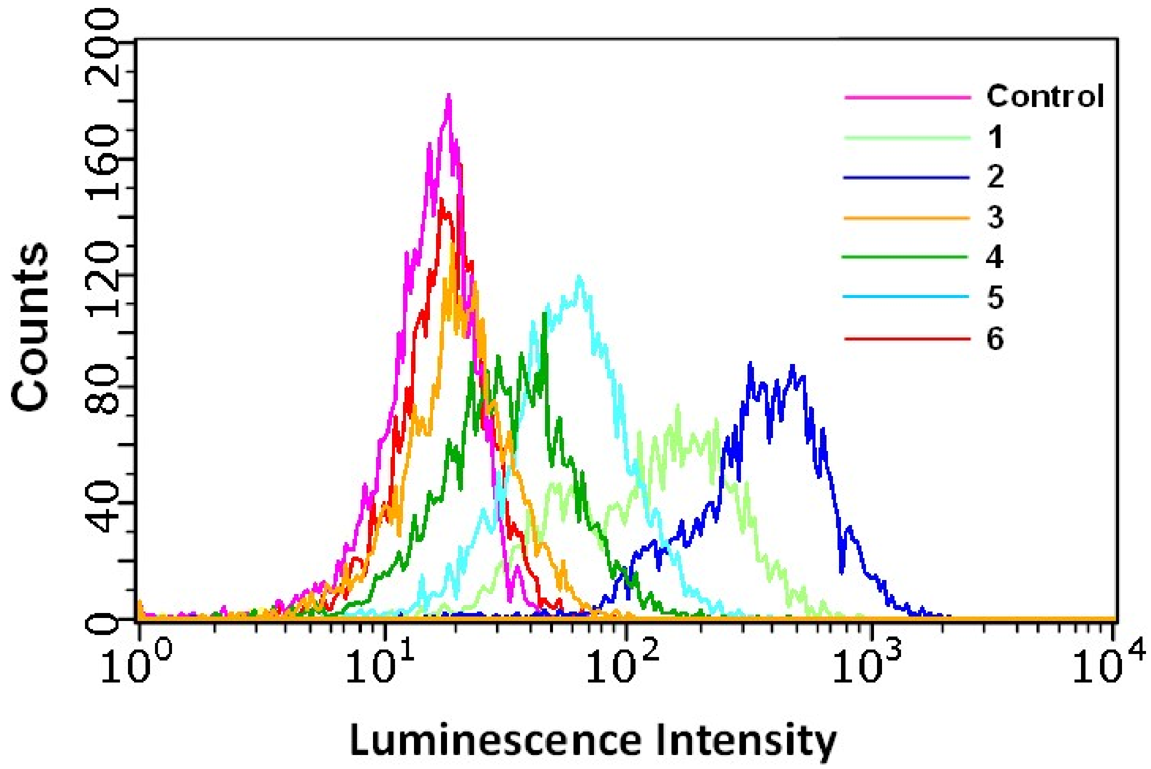

Figure S12. Western blot analysis of the expressions of apoptosis related proteins of human breast (MCF-7) cancer cell line with or without treatment of complex **1** (5 μM), cisplatin (50 μM), and UV light for 24 h.

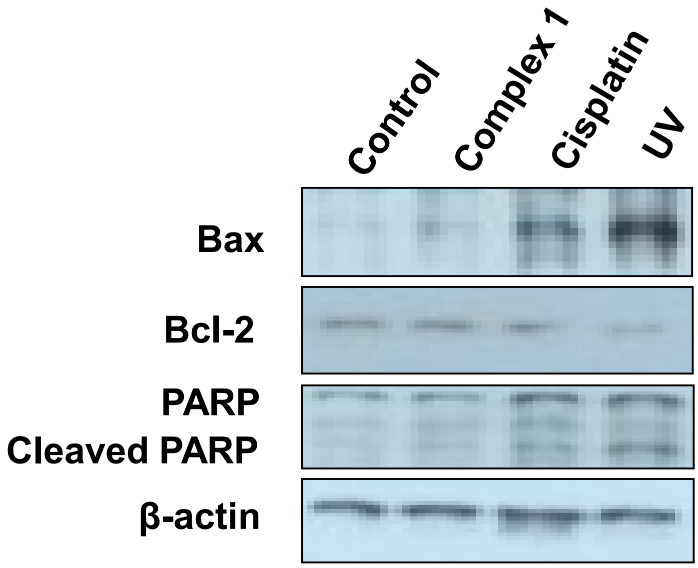

Figure S13. Cell cycle analysis of human breast (MCF-7) cancer cell line with or without treatment of complex **1** at indicated concentrations after 24 h.

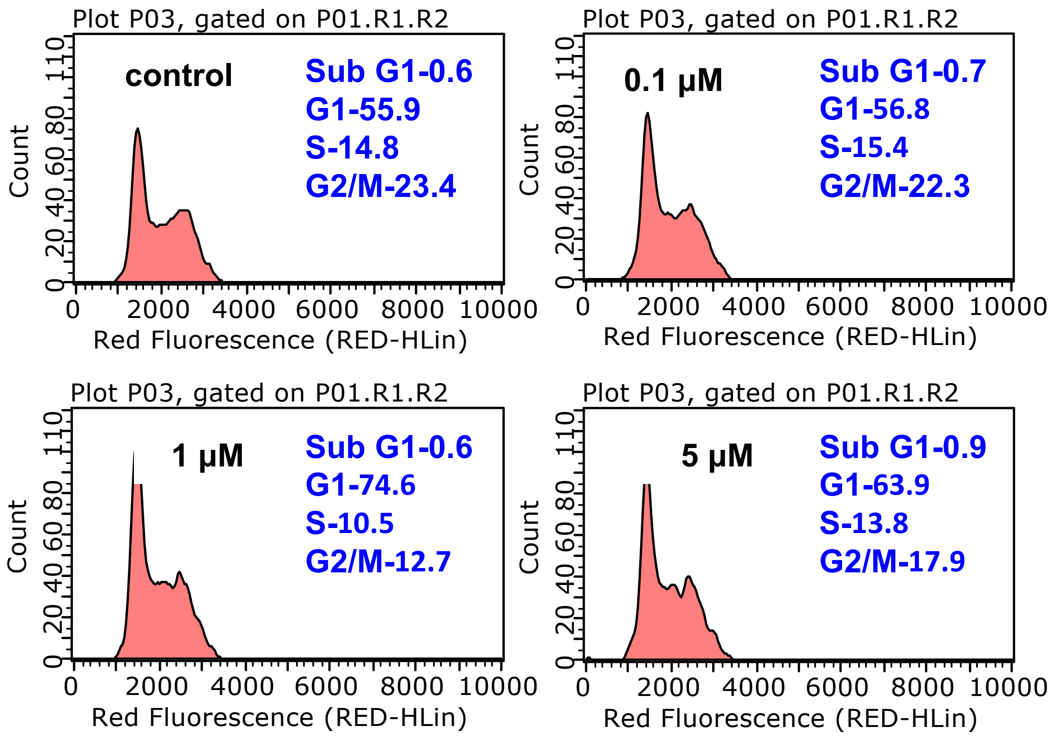

Figure S14. (a) Flow cytometric analysis and (b) fluorescence microscopic images of ROS production incubated with blank medium, only complex **1** (5 μM), complex **1** + MnTBAP (100 μM) and only H_2O_2 (50 μM) at 37 °C for 12 h. (excitation, 488 nm; emission, 530 nm).

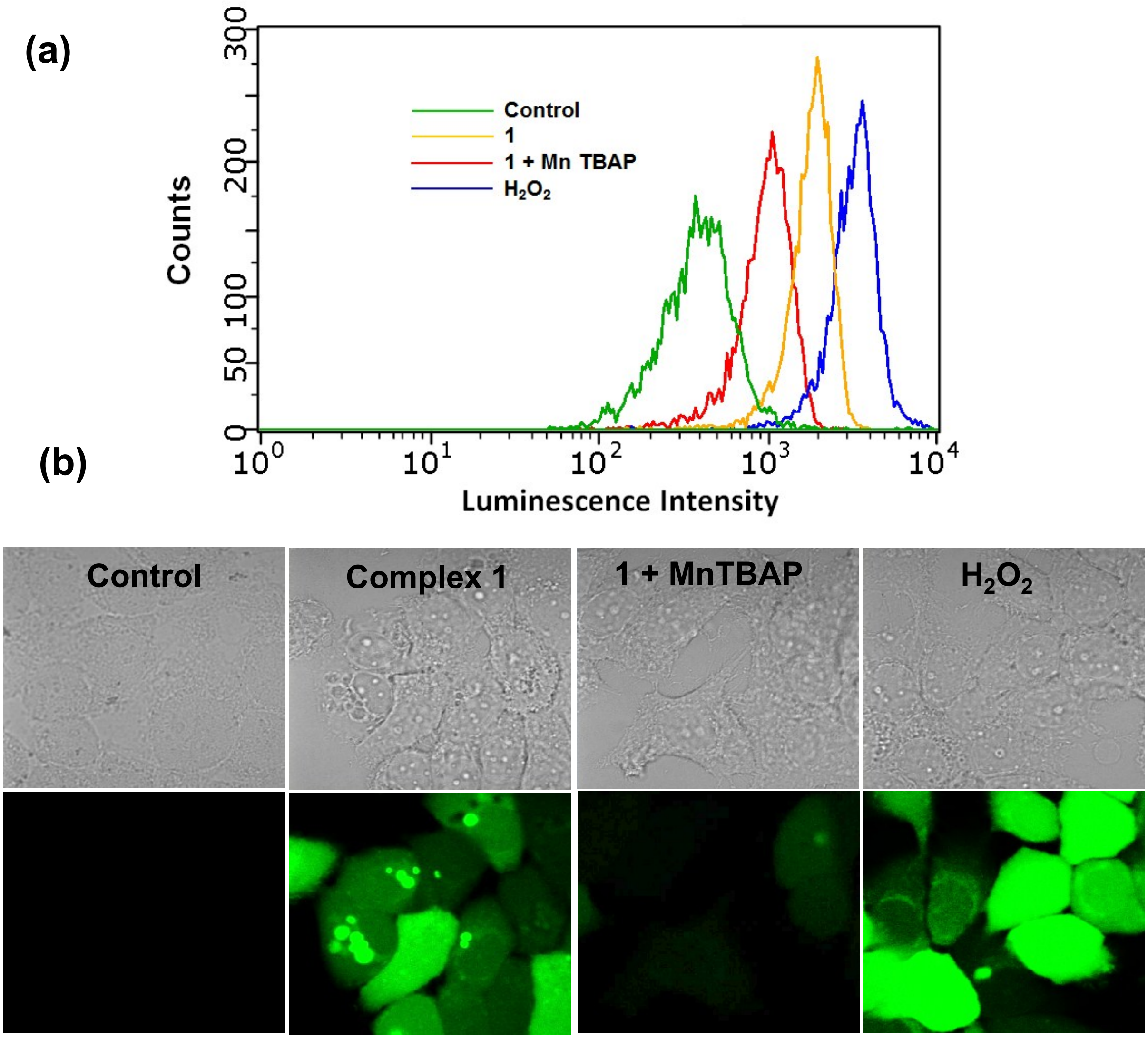

Figure S15. Dose dependent suppression of cell viability of complex **1** towards human breast (MCF-7), prostate (LNCap, PC3, DU145) endometrial (Ishikawa) and Ovarian (SKOV3) cancer cell lines.

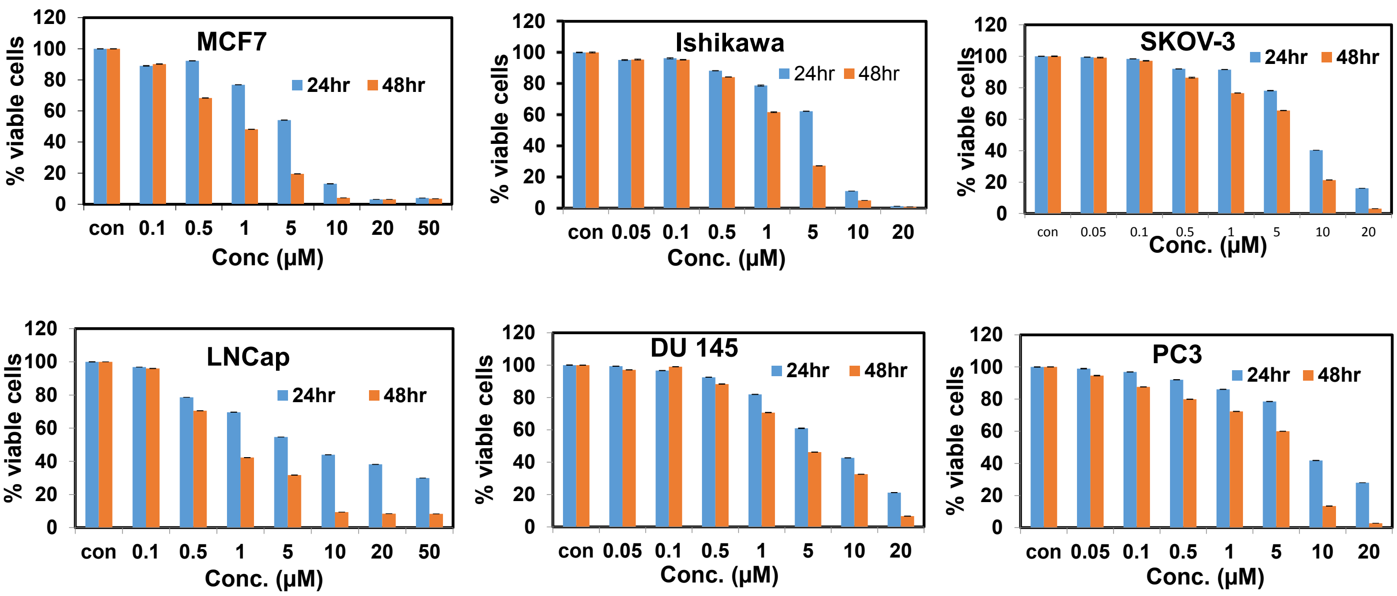

Figure S16. Time dependent western blot analysis of p53 protein expression of human breast (MCF-7), endometrial (Ishikawa) and ovarian (SKOV3) cancer cell lines after the treatment of complex **1** (5 μM).

Figure S17. Florescence microscopic images of human breast (MCF-7) cancer cells in presence of 3, 3´ -dihexyloxacarbocyanine iodide ($DIOC_6$) (40 nM), complex **1** (10 μM) and their overlay image after 12 h incubation.

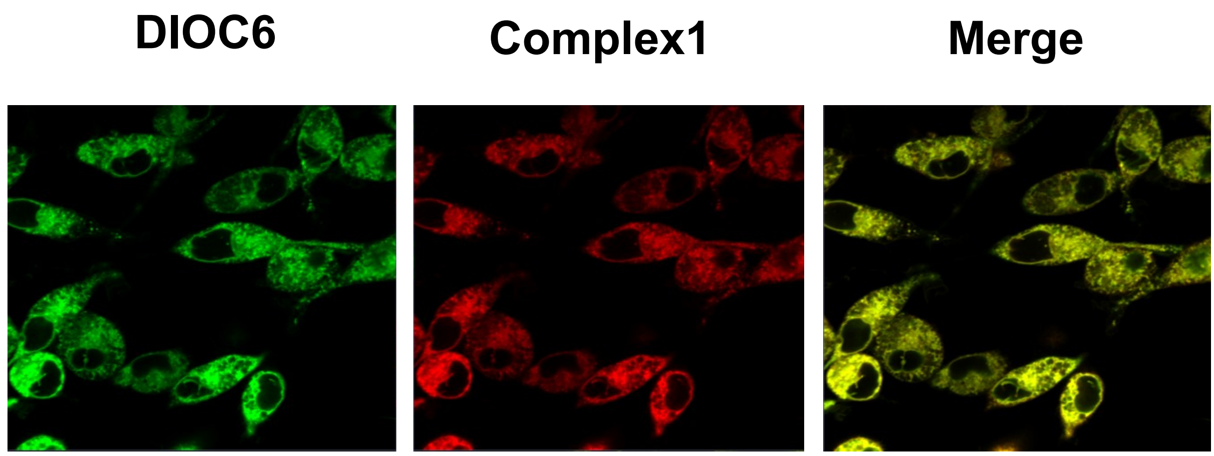
DIOC6
Complex1
Merge